AJAE

Open Access

Vol. 16, No. 1, 2021147, March 2022
doi: https://doi.org/10.5572/ajae.2021.147
ISSN (Online) 2287-1160, ISSN (Print) 1976-6912

Review Article

Review of Atmospheric Environmental Change from Earth Observing Satellites

Kwon-Ho Lee[1)], **Man Sing Wong**[2),3),*], **Jing Li**[2)]

[1)]Department of Atmospheric and Environmental Sciences, Gangneung-Wonju National University (GWNU), Gangneung 25457, Republic of Korea
[2)]Department of Land Surveying and Geo-Informatics, The Hong Kong Polytechnic University, Hong Kong, China
[3)]Research Institute of Land and Space, The Hong Kong Polytechnic University, Hong Kong, China

***Corresponding author.**
Tel: +852-3400-8959
E-mail: Lswong@polyu.edu.hk

Received: 10 December 2021
Accepted: 9 February 2022

ABSTRACT Satellite data is a collection of various atmospheric environmental information through continuous earth observations. Those data observed for a long time-series provide detailed information on environmental changes which has been processed as two-dimensional information representing the atmospheric columnar integrated properties or multi-dimensional data combining space and time. In this review, we investigate the characteristics of various earth observing satellites that have been deriving the global atmospheric information up to date. In terms of applications, the patterns of global atmospheric environmental changes based on statistical and comparative analysis with the long-term observations are also addressed. The spatio-temporal changes in the atmospheric environmental parameters are discussed, in order to provide a quantitative grasp of the statistical relationship. Finally, future developments are put forward. This information will help to understand the atmospheric environment and climate-related interactions.

KEY WORDS Satellite, Atmospheric environment, Environmental monitoring, Remote sensing, Earth observation

1. INTRODUCTION

The earth's atmosphere has been directly or indirectly affected by both human activities and natural change factors (IPCC, 2014). For example, human activities affect the atmospheric environment by emitting various kinds of particulate matter and gaseous substances through automobiles, heating, or agricultural or production activities (McDuffie *et al.*, 2020; Reddington *et al.*, 2019). As for the natural factors, sand storms in deserts increase dust particles in the atmosphere and volcanic eruptions can release various particulate or gaseous substances into the atmosphere (Liora *et al.*, 2015). In the ocean, micro-organisms in water also act as a factor of climate change by releasing oxides (Cavicchioli *et al.*, 2019; Vallina and Simo, 2007; Leck and Bigg, 2005; Charlson *et al.*, 1987). These issues related to the atmospheric environment are not only specific to an independent local area, but also the adjacent and distant areas caused by intertwined effects. For example, long-range transported air pollutants including desert dust storms, biomass burning smoke, and

industrial air pollution may occur internationally (Hatakeyama *et al.*, 2017; Coulibaly *et al.*, 2015). Under these circumstances, it is becoming more important to understand whether the cause of air pollution is from a local source or the contribution of the long-range transport from the outer boundary. Therefore, it is necessary to estimate the current states and evaluate the air pollution levels by multi-dimensional monitoring.

As an atmospheric environmental monitoring technology, satellite data has been widely used to study the temporal and spatial variables of the atmospheric environment over the past few decades (Kokhanovsky and de Leeuw, 2009; Lee *et al.*, 2009; King *et al.*, 1999). For example, the meteorological satellites such as the NOAA series, the Geostationary Operational Environmental Satellite (GOES), the Geostationary Meteorological Satellite (GMS), METEOSAT, and the Earth Observing System (EOS) series have been conducting continuous observation of the global atmosphere (Ackerman *et al.*, 2019). The Earth observing satellites has stimulated the developments in various environmental remote sensing technologies and the production of analytical data. In addition, the analysis techniques using satellite data play an important role in their applications in various fields such as meteorology, air quality, ocean, land cover/land change, agriculture, and so on (Guo *et al.*, 2015). Therefore, the purpose of this study is to review the characteristics of various Earth observing satellites providing environmental big data and processing techniques for obtaining environmental parameters. This study introduces the theoretical principles of characteristics and observation platforms currently used in global environmental monitoring. In addition, by collecting information on the global environment observed for a long time from satellites, the patterns of global environmental changes are also identified based on statistical analysis and comparative analysis results for each parameter.

2. EARTH OBSERVING SATELLITES

The main purpose of earth observation is to enhance the understanding of the global environment and to establish a more effective earth observation system (Anderson *et al.*, 2017). Focusing on this purpose, comprehensive studies of the ocean, atmosphere, land, climate, vegetation, diseases, and disasters have been carried out through many earth observation platforms (Dowman and Reuter, 2016). In order to maximize the utilization of Earth observing satellite, practical efforts such as presentation of data policies, collaborations among international researchers, operation of data centers, and holding of periodic science meetings have been deployed. For example, the Megacity (Zhu *et al.*, 2012) or the Asian Brown Cloud (ABC) programs (Nakajima *et al.*, 2007; Ramanathan *et al.*, 2005) by the International Global Atmospheric Chemistry (IGAC) are international joint observation programs using satellite data for comprehensive analysis on environmental monitoring.

For a better understanding of the global environment,

Table 1. Representative satellite sensors used to observe the atmospheric environment.

Sensor	Platform	Spectral range	Observation parameters
AVHRR	NOAA Series	5 Channels (Vis–IR)	Aerosol, cloud, vegetation, SST
TOMS	Nimbus-7, Meteor, EP, ADEOS, QuickTOMS	UV	O_3, absorbing aerosol
SeaWiFS	SeaSTAR	8 Channels (Vis–NIR)	Aerosol, ocean color, aerosol type, cloud, land cover
MISR	TERRA	4 Channels (Vis–NIR)	Aerosol, cloud, temperature, ocean color, vegetation, land cover
MODIS	TERRA	36 Channels (Vis–IR)	
GLI	ADEOS-2	36 Channels (Vis–IR)	
MERIS	ENVISAT	15 Channels (Vis–IR)	
SCIAMACHY	ENVISAT	Hyperspectral (UV–IR)	Atmospheric trace gases, aerosol, cloud, limb sounding

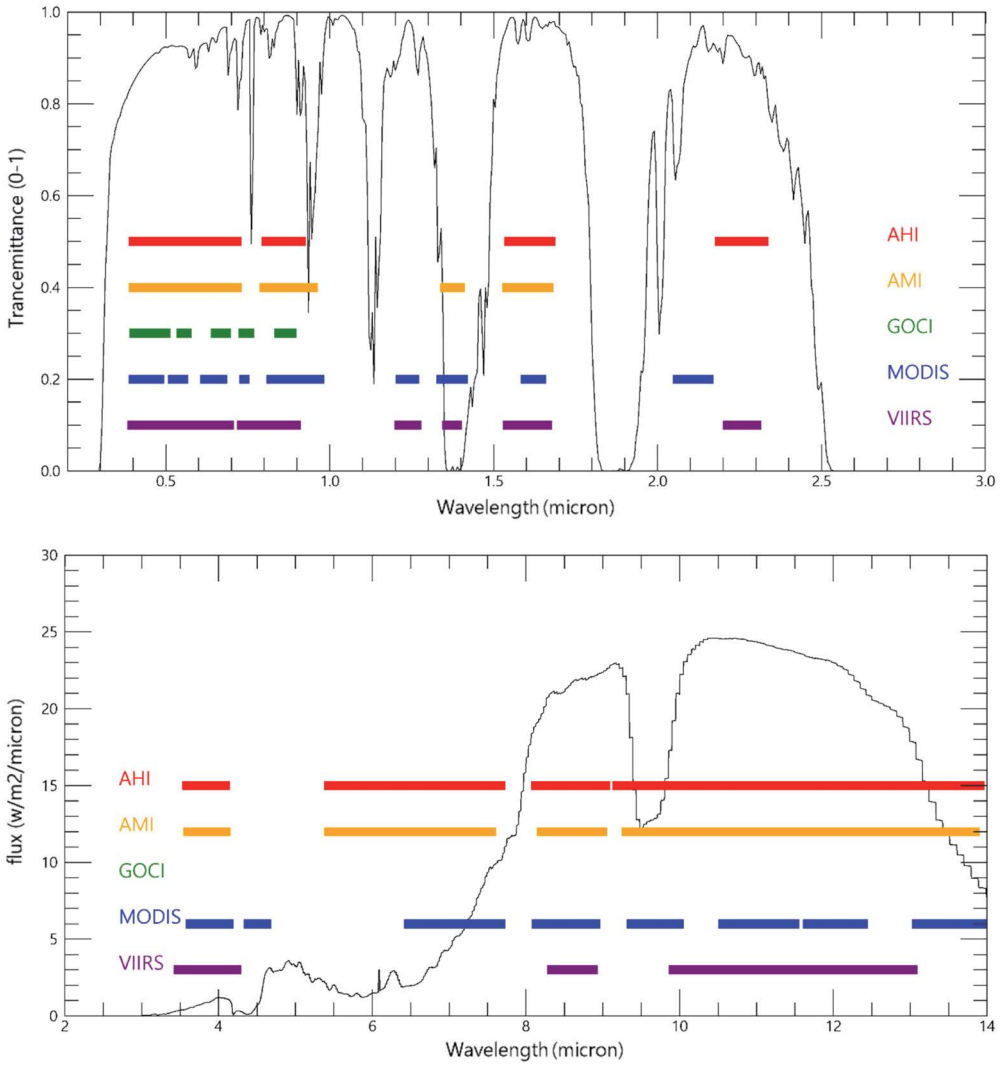

Fig. 1. Spectral band positions across the sensors alongside those of missions for atmospheric environment monitoring. The black line is solar transmittance and flux from LOWTRAN. AHI - Advanced Himawari Imager on Himawari 8/9 (Japan), AMI - Advanced Meteorological Imager on GEO-KOMPSAT2 (South Korea), MODIS - Moderate Resolution Imaging Spectroradiometer (United States).

satellite observations are inevitable because satellites provide a wide range of data on the Earth's environment. Representative examples of satellites include EOS, Environment Satellite (ENVISAT), and Advanced Earth Observing Satellite (ADEOS) series as listed in Table 1. These Earth observing satellites have been widely used for global environmental monitoring and output data have been rapidly increased in all fields such as geographic information, military information, resource exploration, environmental observation, and global climate change prediction. For example, the surface temperature of land and ocean, primary production, land cover, clouds, aerosols, water vapor, temperature, and forest fires have been observed for a long time, and the scientific information produced has played an important role in environmental protection and policy making (Dowman and Reuter, 2016).

More recently, new generation sensors aboard polar orbit satellites and geostationary orbit satellites play a large role in planetary monitoring. The capabilities of these sensors have been greatly improved in terms of spectral spectrum, radiometry, observation time, and scanning speed. For example, the new generation sensors onboard the most recently launched geostationary satellites, such as Advanced Baseline Imager (ABI) on the Geostationary Operational Environmental Satellite-R (GOES-R) series of satellites (Schmit *et al.*, 2017, 2005), Advanced Hima-

wari Imager (AHI) on the Himawari series (Bessho *et al.*, 2016), and Advanced Meteorological Imager (AMI) on the Cheollian satellites (Kim *et al.*, 2021; Jee *et al.*, 2020), have three times more spectral channels, four times better spatial resolution, and five times faster scanning speeds than the previous meteorological sensors. The advanced sensors offer great opportunities for instant and continuous monitoring of acute and extensive disasters (e.g., dust storms, wind storms, and volcanic abruptions). Fig. 1 shows the wavelength range of the three sensors along with typical satellite sensors.

The development of sensor technology has greatly enhanced the ability of satellite data applications. For example, ENVISAT is one of the representative Earth observing satellites and can obtain environmental observation data from 10 onboard sensors. Among these sensors, Scanning Imaging Absorption Spectrometer for Atmospheric ChartY (SCIAMACHY) is a spectrometer that measures sunlight with a wavelength resolution of (0.2 to 1.5 nm) in the ultraviolet-near infrared region (240 nm to 2,380 nm) which can measure atmospheric constituents. In addition, Ozone Monitoring Instrument (OMI), The TROPOspheric Monitoring Instrument (TROPOMI), etc. can observe various types of gases, aerosols, radiation, clouds, and cloud altitudes (Fig. 2).

One of the oldest earth observing satellites currently in operation is the EOS-AM1 (Terra) satellite, which was launched on December 18, 1999. It has been collecting various earth observing data and analysing the impact of human activities on global environmental changes. The EOS-PM1 (Aqua) satellite, launched in 2001, is the successor to the Terra Earth Observation Satellite. Both EOS satellites have been used to identify seasonal cycles of ecosystems in land and ocean, to detect seasonal changes in the atmosphere and clouds, and to calculate the daily surface temperature of the globe regardless of weather conditions. Among the various sensors mounted on the EOS satellites, the MODerate Resolution Imaging Spectroradiometer (MODIS) (Barnes *et al.*, 2003; Pagano and Durham, 1993) is a multi-spectral radiometer that measures radiation energy in the visible to long-wave infrared wavelength region at intervals of about 1.478 seconds. The observation range of MODIS is between −55 degrees west to + 55 degrees east, which corresponds to a range of about 2,330 km on the ground (cross track), and it can scan an area of about 10 km in the direction of the satellite (along track). The EOS satellites orbit the Earth's polar orbit once for about 100 minutes, and it orbits about 14.4 times a day, so it takes about 2 days to scan the entire Earth. MODIS has a total of 36 channels, among which 2 channels (640 nm, 860 nm) with a resolution of about 250 m at nadir view, 5 channels with a resolution of 500 m (470 nm, 555 nm, 1,240 nm, 1,640 nm, 2,130 nm), and 29 channels with a resolution of 1 km. About 20 channels out of 36 measure in the spectrum of reflected sunlight, and the others measure in those of infrared.

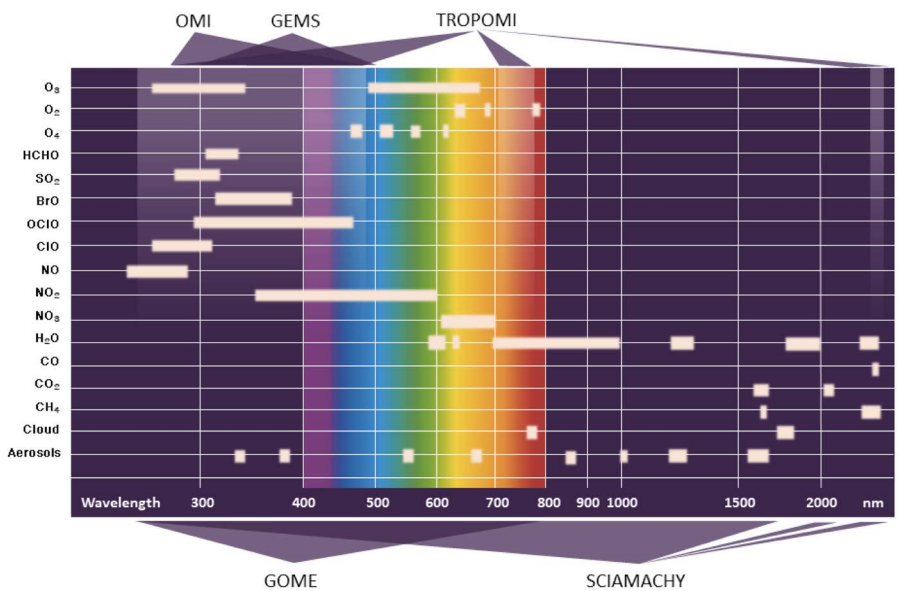

Fig. 2. Spectral ranges for hyperspectral sensors including GEMS, GOME, OMI, SCIAMACHY, and TROPOMI.

3. ATMOSPHERIC ENVIRONMENT MONITORING FROM EOS

Satellite observations have become a means to complement the existing computational numerical models by providing information on the status and behaviour of atmospheric aerosols and clouds. The aerosol-related physical quantity commonly used in satellites is the aerosol optical thickness (AOT), which means the amount of radiation attenuated by the aerosol particles in the atmosphere. In general, AOT is determined by analysing the radiative transfer process of the reflected light of the sun in the visible region. The following Eq. (1) is widely used for the radiative transfer process by the Earth's atmosphere and surface in the visible wavelength range:

$$\rho_{TOA}(\tau) = \rho_{Aer}(\tau) + \rho_{Ray}(p,t) + \frac{T_0(\tau_{gas})\cdot T_S(\tau_{gas})\cdot \rho_{Sfc}}{1-\rho_{Sfc}\cdot r_h(\tau)} \quad (1)$$

where, ρ_{TOA}, ρ_{Aer}, ρ_{Ray}, and ρ_{Sfc} are the reflectance observed by the satellite sensor at the top of the atmosphere, the reflectance by atmospheric aerosol, the reflectance by the molecules in the atmosphere, and the reflectance by the ground surface, respectively. T_{Sun} and T_{Sat} are the atmospheric transmittance corresponding to the path from the target point observed by the satellite to the sun and the satellite, respectively. r_{Hem} is the reflectivity due to the atmospheric hemisphere. λ, τ represent wavelength and AOT, respectively. Basically, the AOT is determined from the relationship between τ and ρ_{Aer} which can be acquired by deducting the molecular and surface reflectance terms from ρ_{TOA}. Based on this process, various types of aerosol retrieval algorithms were developed (Lee *et al.*, 2009).

On the other hand, Eq. (1) uses scattered light, there are a few algorithms that use the differential absorption of the aerosols for ultraviolet (UV) or infrared (IR) channels. These methods use the various functions of difference or ratios derived from the sensitive and insensitive wavelengths to the absorption of aerosol, e.g.,

$$I(\tau) \cong f(L_{nabs} - L_{abs}) \quad (2)$$

$$I(\tau) \cong f\left(\frac{Lnabs}{Labs}\right) \quad (3)$$

where I, L_{abs} and L_{nabs} are the derived index for absorbing aerosols, radiance of absorbing aerosols, and non-absorbing aerosols, respectively. It is worth noting that the index value is expressed in various ways depending on the algorithm (Li *et al.*, 2021).

Additionally, the thermal infrared (TIR) spectrum is preferentially sensitive to the coarse-mode aerosol particles (Peyridieu *et al.*, 2010). The TIR has been implemented for retrieving large aerosol particles, such as dust (Zhang *et al.*, 2006) and volcanic ash aerosols (Wen and Rose, 1994). The satellite sensor captured thermal radiances consisting of two parts, the radiance emitted from the aerosol (e.g., dust, volcanic ash) cloud layer and the radiance emitted from the underlying surface. The radiative transfer process at thermal spectra can be approximated as:

$$I_i \approx t_i B(T_s) + \varepsilon_i B(T_c) \quad (4)$$

where I_i is the observed radiance at the top of the atmosphere (TOA), t_i and ε_i are the transmissivity and emissivity of the cloud layer at wavelength *i*. T_s and T_c indicate the underlying surface temperature and the top temperature of the cloud layer. The *B* stands for the Plank function. $B(T_s)$ and $B(T_c)$ are the blackbody radiances at equivalent temperatures of T_s and T_c. The emissivity of the underlying surface is assumed to be 1 in Eq. (4). Both the transmissivity and emissivity of the cloud layer are determined by the optical depth τ_i and they are expressed as:

$$\varepsilon_i = 1 - e^{-\tau_i} \quad (5)$$

$$t_i = e^{-\tau_i} \quad (6)$$

According to Eqs. (4), (5), and (6), the satellite observed radiance is strongly controlled by the underlying surface, cloud temperature, and optical depth of the aerosol layer. Therefore, the AOT can be inversely calculated if the TOA radiance has been obtained and T_s and T_c have been fixed.

Table 2 summarizes the aerosol retrieval algorithms which have been developed according to the operating purpose and characteristics of each satellite sensor.

To remove (or minimize) the effect of surface reflection, the aerosol retrieval methods listed in Table 2 generally use background images (e.g., clearest images with very high atmospheric transmittance) or dark surface reflectance in the specific channels (e.g., near-infrared channels in seawater, blue and red channels in areas with dense vegetation, etc.). After removing the influence of surface reflection, the satellite signal is then converted into the physical quantity of aerosol using the pre-calculated look-up tables (LUTs).

Table 2. Summary of major satellite aerosol retrieval methods.

Method	Principles	Satellite	Reference
1-channel	Low surface reflectance only LUT	NOAA/AVHRR series	Rao *et al.* (1989), Stowe (1991)
2-channels	Low surface reflectance only LUT	NOAA/AVHRR series	Stowe *et al.* (1997), Mishchenko *et al.* (1999)
UV- Absorbing	UV spectral range only LUT	TOMS series	Hsu *et al.* (1996), Herman *et al.* (1997), Torres *et al.* (2002)
Ocean color	Low surface reflectance at longer visible wavelengths only LUT	CZCS, SeaWiFS, OCTS, MODIS	Gordon and Wang (1994)
Polarization	Directional polarization LUT	POLDER series	Herman *et al.* (1997), Deuze *et al.* (1999), Breon *et al.* (2002)
Multi-channel	Dark target LUT	SeaWiFS, MODIS, MERIS	Kaufman *et al.* (1997), Remer *et al.* (2005), von Hoyningen-Huene *et al.* (2006, 2005)
Multi-angle	Dark target LUT	MISR	Diner *et al.* (1998)
Thermal-Infrared	Highest brightness temperature LUT	MODIS	Zhang *et al.* (2006)

One of the important environmental measurements of the EOS program is the observation of atmospheric aerosols and clouds. Earth observing satellites prior to MODIS were difficult to observe aerosols over bright surfaces, mainly due to the limitations of the number of observation channels. MODIS made it possible to observe aerosols with improved spectral resolution. One of the characteristics of the MODIS aerosol retrieval method is to determine the visible channel surface reflectance by using both background image and dark surface methods. The "Deep Blue" and "Dark Target" methods use a background surface reflectance and a change rate for each wavelength, respectively (Levy *et al.*, 2013; Hsu *et al.*, 2006; Remer *et al.*, 2005). Another feature is that the aerosol signal is divided into fine mode and coarse mode. The aerosol load and size information are obtained using the calculated look-up tables assuming 11 particle size distributions (5 fine particle modes, 6 coarse particle modes) in 6 bands between 0.55 μm to 2.13 μm. MODIS aerosol products are processed into data (codename: MOD04, MYD04) with a spatial resolution of about 10 km at Level-2 and gridded data at one-degree latitude and longitude intervals at Level-3 (MOD08) format.

Recently, the MODIS aerosol retrieval algorithm has been updated to version 6, and different aerosol products according to the algorithm have been produced. The results of comparing the different MODIS aerosol products over the East Asian region were reported (Lee, 2018). Fig. 3 shows the mean AOT in East Asia observed by MODIS from 2001 to 2016. Statistical distribution of aerosol can be confirmed through this long-term satellite observation result. It clearly shows that the Asian aerosols are mainly caused by carbon particles generated by combustion and sand storms in dry areas (i.e. Gobi Desert, Taklamakan Desert, etc.), and pollutant particles generated in densely populated areas or industrial areas. Moreover, AOT in these areas appears to be in relatively large values.

Fig. 4 shows the long-term trend of AOT from 2001 to 2019. On a global scale, the pattern of AOT clearly shows a seasonal cycle that rises in summer and falls in winter, but a significant increasing or decreasing trend is not found (linear fit slope = 1.996×10^{-4}, Y-intercept = 0.170). On the contrary, the AOT over East Asia (10°S–60°N, 60°E–150°E) is larger than that of the global scale and is showing an increasing trend until 2012 (linear fit slope = 1.879×10^{-4}, Y-intercept = 0.251). After 2013, it shows a slight decrease (linear fit slope = -4.0×10^{-4},

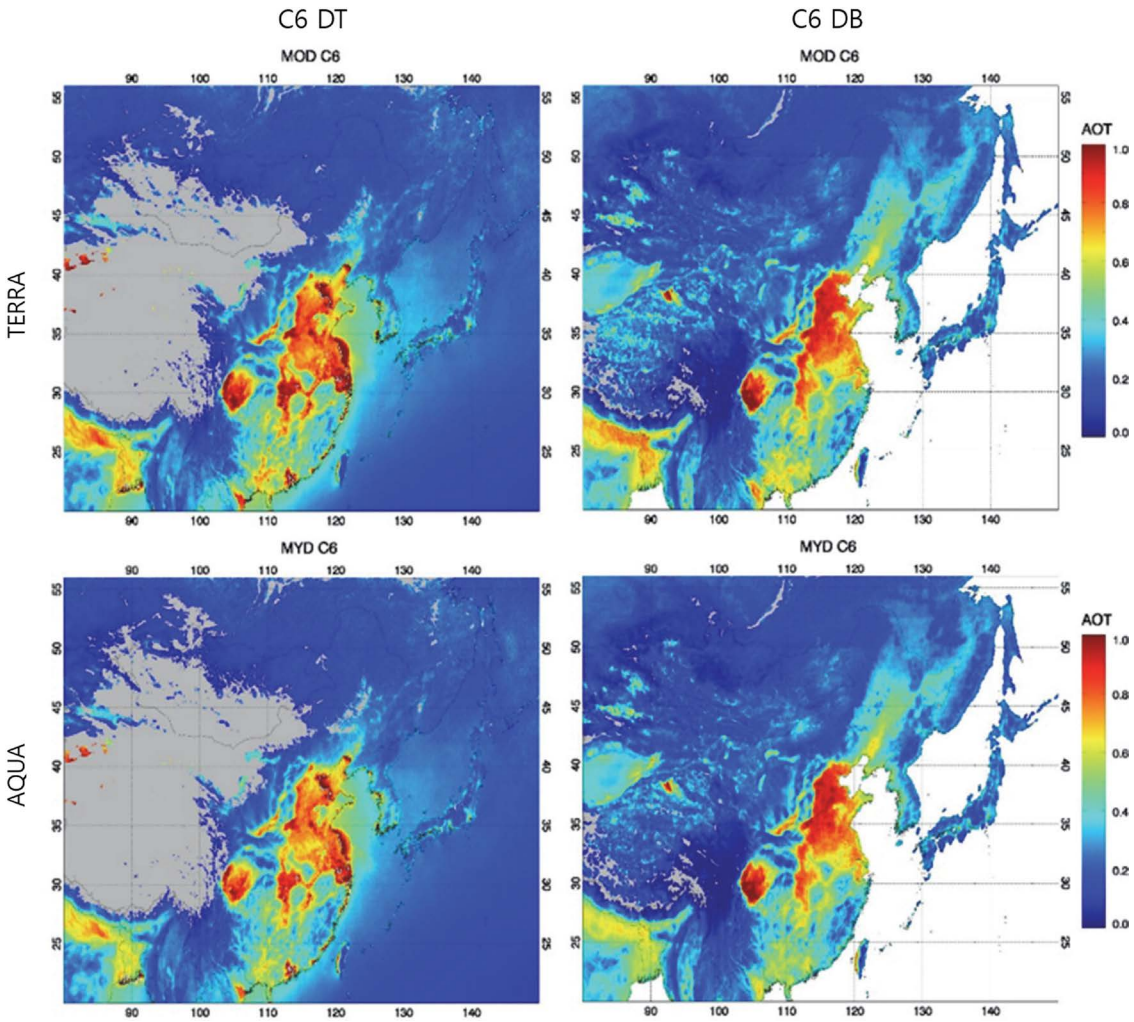

Fig. 3. The averaged spatial distribution of AOT from different collections and retrieval algorithms for MODIS level 2 aerosol products during 2000–2019 (Terra) and 2002–2019 (Aqua), respectively. Note that AOT data from DB algorithm are available over land only.

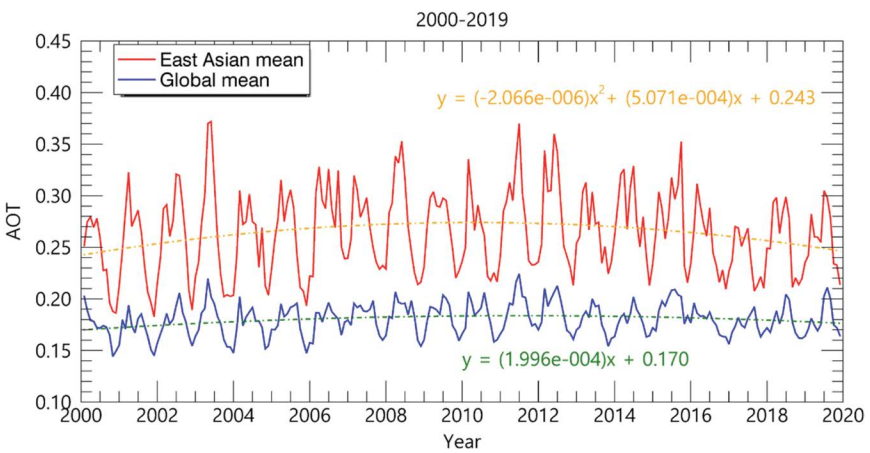

Fig. 4. Time series of area averaged Terra/MODIS AOT over 2000–2019. Second order poly-fit equations are plotted as dashed lines.

Y-intercept = 0.279). Mean AOT values during the whole period are 0.264 ± 0.039 for East Asia and 0.180 ± 0.015 for the globe, that the East Asian mean AOT is about 1.47 times larger than the global average. These regional imbalances and long-term trends in atmospheric aerosols found in East Asia are unique. Therefore, areas with a high load of atmospheric aerosols are known to have a high contribution to atmospheric hydrological circulation and radiation balance (Ramanathan *et al.*, 2001). This mechanism is one of the uncertainty factors in climate change study and is also related to many other mechanisms of climate change that are still not fully understood.

4. EFFECTS ON NATURE

The properties of absorbing or scattering sunlight by aerosol particles differ depending on the chemical composition and physical properties of the aerosol (Myhre, 2009; Forster *et al.*, 2007). Aerosols also interact with cloud and hydrological circulation by acting as cloud condensation nuclei (CCN) and ice nuclei (Seinfeld *et al.*, 2016). While the liquid water content (LWC) is constant, more CCN increases the cloud albedo (indirect cloud albedo effect) (Lohmann and Feichter, 2005) and decreases the precipitation efficiency (indirect cloud lifetime effects) (Koch and Del Genio, 2010; Hansen *et al.*, 1997), reducing the global annual average of net radiation at the top of the atmosphere. However, these effects may be partially offset by evaporation of cloud particles due to aerosols (indirect effects) and more ice nuclei (glacial effects). In addition, the surface can be cooled due to the lack of incoming solar radiation, while the boundary layer can be warmed by absorption of solar radiation; interaction between the two systems can increase thermal stability and reduce cloud formation, thereby reducing rainfall. Menon *et al.* (2002) stated that the presence of pollution particles mainly composed of carbon components in the Asian atmosphere exhibits a cooling effect of the surface by scattering or absorbing sunlight, which is approximately three times larger than the greenhouse effect.

Atmospheric aerosols are directly or indirectly related to climate, and eventually affect terrestrial organisms. Specifically, both the clouds and aerosols can exert influences on the surface vegetation. On one hand, the presence and interaction of aerosols and clouds can block sunlight reaching the surface and thus reduce the amount of light energy required for photosynthesis of plants. On the other hand, photosynthesis and evaporation may rather increase with more scattered rays by aerosols and clouds. Therefore, it is critical to analyse the relationship between the aerosols and clouds in the Earth's atmosphere with climate change and environmental change. Several indicators have been developed to quantify the respective properties of aerosols, clouds, and vegetations, including the Angstrom Exponent (AE), Cloud Effective Radius (CER), and Normalized Difference Vegetation Index (NDVI). The AE describes how the AOT depends on the wavelength of the light (Ångström, 1929). For τ_1 and τ_2 at two different wavelengths of λ_1 and λ_2, the AE is given by;

$$AE = -\frac{ln\frac{\tau_1}{\tau_2}}{ln\frac{\lambda_1}{\lambda_2}} \tag{7}$$

It is typically used as a relative indicator of aerosol size, with larger values indicating small particles, and smaller values indicating large particles. The CER is a weighted mean of the size distribution of cloud droplets which is typically used in cloud remote sensing (Hansen and Trevis, 1974). It is expressed as;

$$CER = \frac{\int_0^\infty \pi \cdot r^3 \cdot n(r)}{\int_0^\infty \pi \cdot r^2 \cdot n(r)} \tag{8}$$

CER data from satellite remote sensing has been widely used for estimating aerosol-cloud interactions (Ross *et al.*, 2018; Menon *et al.*, 2008) and cloud feedback (Tan *et al.*, 2019). NDVI is generally used to quantify vegetation density by measuring the difference reflection between near-infrared (which vegetation strongly reflects) and red light (which vegetation absorbs). It is calculated as the difference between near-infrared (NIR) and red (RED) reflectance (ρ_{NIR} and ρ_{Red}) divided by their sum.

$$NDVI = \frac{\rho_{NIR} - \rho_{Red}}{\rho_{NIR} + \rho_{Red}} \tag{9}$$

NDVI ranges from −1.0 to 1.0. Values close to one represents green vegetation dominated; values close to zero are mainly caused by soil or rocks; negative values are primarily formed from clouds, water, and snow. Multitemporal profiles of the satellite-based NDVI has been widely used to study their seasonal phenologies (Huete *et al.*, 2002).

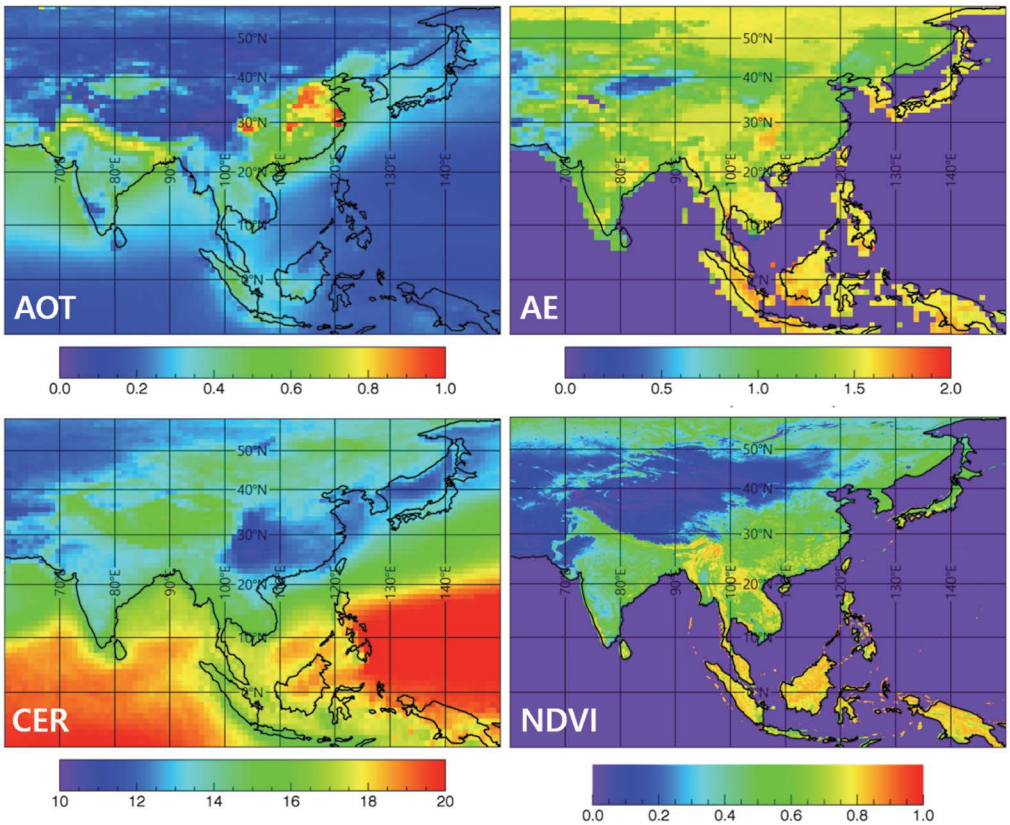

Fig. 5. Mean AOT, AE, CER, and NDVI during 2000–2019 from Terra/MODIS.

Fig. 5 displays the averaged AOT, AE, CER, and NDVI collected from the Terra/MODIS during 2000–2019. It highlights the heavy pollution over India and East Asia, biomass burning smokes over Southeast Asia, and large dust aerosols over desert regions. East Asia exhibits a high aerosol level, while a relatively low CER compared to other regions. These results prove that the interaction between aerosols and clouds has strong regional variations.

Given that aerosol can have a serious impact on regional-scale climate, a correlation analysis between aerosol and cloud, aerosol, and vegetation distribution is performed. In this analysis, pixel values with the same latitude and longitude in every year are used to derive a linear regression between the two selected variables. Such analysis can reveal the temporal association between those variables at a numerical level. Fig. 6 shows the results of correlation analysis between aerosol, cloud, and vegetation indices. Compared to Fig. 5, it is found that in light aerosol-loaded regions, the AOT has positive relationships with both CER and NDVI (Fig. 6), revealing a positive relationship between CER and NDVI as well; in heavy aerosol-loaded regions, the AOT exhibit negative relationships with both CER and NDVI (Fig. 6) and thus CER is uncovered to retain the positive relationship with NDVI. The above findings imply that an increase of AOT can lead to an increase of vegetation under the light-aerosol-loaded situation, but a decrease of vegetation under the heavy-aerosol-loaded situation. Whereas, an increase of clouds can constantly enhance vegetation density under both situations.

5. SUMMARY AND CONCLUSION

Due to the various air pollution events including sand dust storms occurring in dry areas, forest fires and biomass burning activities, and air pollutants emitted from densely populated/industrialized areas, an effective atmospheric environmental monitoring is required. Especially, air pollution in these East Asian regions has been reported as it had been rapidly increased until the early 2000s

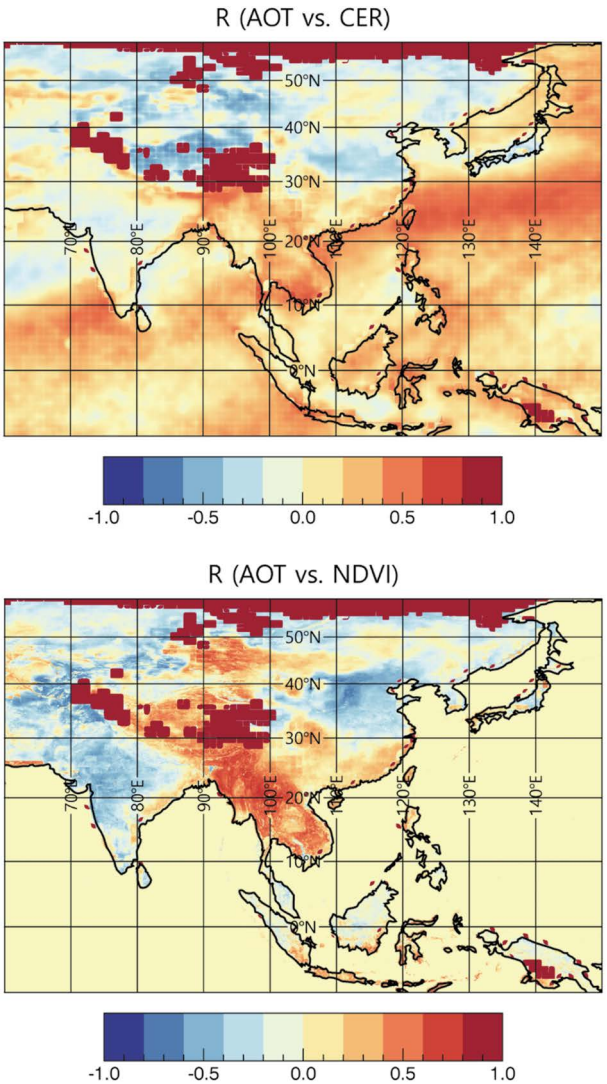

Fig. 6. Linear regression coefficients derived from the monthly (upper) AOT with CER and (lower) AOT with NDVI.

(Akimoto, 2003). The satellite observation provides visualized information on these atmospheric environmental phenomena by retrieval of the physical parameters, and provides information on the emission sources and the transport pathways of pollutants. By using past or currently operating earth observing satellites, information on aerosols and clouds as well as other environmental parameters can be obtained, which is useful for monitoring the atmospheric environment. Those earth observing satellites are expected to provide an opportunity to solve various environmental issues on earth.

Moreover, earth observing satellites are a collection of cutting-edge complex sciences and technologies of system planning, design, manufacturing, operation, and utilization. Unique environmental products have been produced from the various earth observing satellites, so users can find the data suitable for their purposes. Especially, recent geostationary satellites launched in Asia, Europe, and the United States are used to build a nationwide environmental monitoring network, producing scientific research results. Moreover, if research activities on design and data use for integrated environmental observation are actively carried out, it is expected that the ripple effect will be great for the research fields of local air pollution and global-scale climate change. In addition, it is expected that if technology research on disaster prediction and pollution forecasting is conducted, it will not only improve air pollution in Northeast Asia, but also encourage economic cooperation.

ACKNOWLEDGEMENT

This research was supported by Basic Science Research Program through the National Research Foundation of Korea (NRF) funded by the Ministry of Education (NRF-2019R1I1A3A01062804). M.S. Wong would like to acknowledge the funding support from the General Research Fund (Grant No. 15603920 and 15609421), and Collaborative Research Fund (Grant No. C7064-18GF), Hong Kong Research Grants Council, China.

REFERENCES

Ackerman, S., Platnick, S., Bhartia, P., Duncan, B., L'Ecuyer, T., Heidinger, A., Skofronick-Jackson, G., Loeb, N., Schmit, T., Smith, N. (2019) Satellites see the World's Atmosphere. Meteorological Monographs, 59(1), 4.1–4.53. https://doi.org/10.1175/AMSMONOGRAPHS-D-18-0009.1

Akimoto, H. (2003) Global Air Quality and Pollution. Science, 302, 1716–1719.

Anderson, K., Ryan, B., Sonntag, W., Kavvada, A., Friedl, L. (2017) Earth observation in service of the 2030 agenda for sustainable development. Geo-spatial Information Science, 20(2), 77–96. https://doi.org/10.1080/10095020.2017.1333230

Ångström, A. (1929) On the Atmospheric Transmission of Sun Radiation and on Dust in the Air. Geografiska Annaler, 11, 156–166. https://doi.org/10.2307/519399

Barnes, W.L., Xiong, X., Guenther, B.W., Salomonson, V. (2003) Development, characterization, and performance of the EOS MODIS sensors. Proceeding of SPIE 5151. Earth Observing Systems VIII, (10 November 2003). https://doi.org/10.

1117/12.504818

Bessho, K., Date, K., Hayashi, M., Ikeda, A., Imai, T., Inoue, H., Kumagai, Y., Miyakawa, T., Murata, H., Ohno, T., Okuyama, A., Oyama, R., Sasaki, Y., Shimazu, Y., Shimoji, K., Sumida, Y., Suzuki, M., Taniguchi, H., Tsuchiyama, H., Uesawa, D., Yokota, H., Yoshida, R. (2016) An Introduction to Himawari-8/9 Japanese New-Generation Geostationary Meteorological Satellites. Journal of the Meteorological Society of Japan, Ser. II, 94(2), 151–183. https://doi.org/10.2151/jmsj.2016-009

Breon, F.M., Tanre, D., Generoso, S. (2002) Aerosol effect on cloud droplet size monitored from satellite. Science, 295, 834–838. https://doi.org/10.1126/science.1066434

Cavicchioli, R., Ripple, W.J., Timmis, K.N., Azam, F., Bakken, L.R., Baylis, M., Behrenfeld, M.J., Boetius, A., Boyd, P.W., Classen, A.T., Crowther, T.W., Danovaro, R., Foreman, C.M., Huisman, J., Hutchins, D.A., Jansson, J.K., Karl, D.M., Koskella, B., Mark, W., David, B., Martiny, J.B.H., Moran, M.A., Orphan, V.J., Reay, D.S., Remais, J.V., Rich, V.I., Singh, B.K., Stein, L.Y., Stewart, F.J., Sullivan, M.B., van Oppen, M.J.H., Weaver, S.C., Webb, E.A., Webster, N.S. (2019) Scientists' warning to humanity: microorganisms and climate change. Nature Reviews Microbiology, 17, 569–586. https://doi.org/10.1038/s41579-019-0222-5

Charlson, R.J., Lovelock, J.E., Andreae, M.O., Warren, S.J. (1987) Oceanic phytoplankton, atmospheric sulphur, cloud albedo and climate. Nature, 326, 655–661. https://doi.org/10.1038/326655a0

Coulibaly, S., Minami, H., Abe, M., Hasei, T., Oro, T., Funasaka, K., Asakawa, D., Watanabe, M., Honda, N., Wakabayashi, K., Watanabe, T. (2015) Long-range transport of mutagens and other air pollutants from mainland East Asia to western Japan. Genes and Environment: the Official Journal of the Japanese Environmental Mutagen Society, 37(25). https://doi.org/10.1186/s41021-015-0025-5

Deuzé, J.L., Herman, M., Goloub, P., Tanré, D., Marchand, A. (1999) Characterization of aerosols over ocean from POLDER/ADEOS-1. Geophysical Research Letters, 26(10), 1421–1424. https://doi.org/10.1029/1999GL900168

Diner, D.J., Beckert, J.C., Reilly, T.H., Bruegge, C.J., Conel, J.E., Kahn, R.A., Martonchik, J.V., Ackerman, T.P., Davies, R., Gerstl, S.A.W., Gordon, H.R., Muller, J.P., Myneni, R.B., Sellers, P.J., Pinty, B., Vertraete, M.M. (1998) Multi-angle imaging Spectro Radiometer (MISR) instrument description and experiment overview. IEEE Transactions on Geoscience and Remote Sensing, 36, 1072–1087. https://doi.org/10.1109/36.700992

Dowman, I., Reuter, I. (2016) Global geospatial data from Earth observation: status and issues. International Journal of Digital Earth, 10, 328–341. https://doi.org/10.1080/17538947.2016.1227379

Forster, P., Ramaswamy, V., Artaxo, P., Berntsen, T., Betts, R., Fahey, D.W., Haywood, J., Lean, J., Lowe, D.C., Myhre, G., Nganga, J., Prinn, R., Raga, G., Schulz, M., Van Dorland, R. (2007) Changes in Atmospheric Constituents and in Radiative Forcing. In Climate Change 2007: The Physical Science Basis. Contribution of Working Group I to the Fourth Assessment Report of the Intergovernmental Panel on Climate Change (Solomon, S., Qin, D., Manning, M., Chen, Z., Marquis, M., Averyt, K.B., Tignor, M. and Miller, H.L. Eds), Cambridge University Press, Cambridge, United Kingdom and New York, NY, USA.

Gordon, H.R., Wang, M. (1994) Retrieval of water-leaving radiance and aerosol optical thickness over the oceans with SeaWiFS: A preliminary algorithm. Applied Optics, 33, 443–452. https://doi.org/10.1364/AO.33.000443

Guo, H.D., Zhang, L., Zhu, L.W. (2015) Earth observation big data for climate change research. Advanced Climate Change Research, 6, 108–117. https://doi.org/10.1016/j.accre.2015.09.007

Hansen, J.E., Sato, M., Ruedy, R. (1997) Radiative forcing and climate response. Journal of Geophysical Research, 102, 6831–6864. https://doi.org/10.1029/96JD03436

Hansen, J.E., Travis, L.D. (1974) Light scattering in planetary atmospheres. Space Science Reviews, 16, 527–610. https://doi.org/10.1007/BF00168069

Hatakeyama, S., Kim, Y.P., Hsiao, T.C., Matsuda, K., Jaffe, D.A. (2017) Preface to Special Issue - Long-range transported air pollutants in East Asia - Observation, measurements, and model analysis. Aerosol and Air Quality Research, 17, I–II. https://doi.org/10.4209/aaqr.2017.12.lrt

Herman, J.R., Bhartia, P.K., Torres, O., Hsu, C., Seftor, C., Celarier, E. (1997a) Global distribution of UV-absorbing aerosols from Nimbus 7/TOMS data. Journal of Geophysical Research, 102, 16911–16922. https://doi.org/10.1029/96JD03680

Herman, M., Deuzé, J.L., Devaux, C., Goloub, P., Bréon, F.M., Tanré, D. (1997b) Remote sensing of aerosols over land surfaces, including polarization measurements; application to some airborne POLDER measurements. Journal of Geophysical Research, 102, 17039–17049. https://doi.org/10.1029/96JD02109

Hsu, N.C., Herman, J.R., Bhartia, P.K., Seftor, C.J., Torres, O., Thompson, A.M., Gleason, J.F., Eck, T.F., Holben, B.N. (1996) Detection of biomass burning dmoke from TOMS measurements. Geophysical Research Letters, 23(7), 745–748. https://doi.org/10.1029/96GL00455

Hsu, N.C., Tsay, S.-C., King, M.D., Herman, J.R. (2006) Deep blue retrievals of Asian aerosol properties during ACE-Asia. IEEE Transactions on Geoscience and Remote Sensing, 44(11), 3180–3195. https://doi.org/10.1109/tgrs.2006.879540

Huete, A., Didan, K., Miura, T., Rodriguez, E.P., Gao, X., Ferreira, L.G. (2002) Overview of the radiometric and biophysical performance of the MODIS vegetation indices. Remote Sensing of Environment, 83, 195–213. https://doi.org/10.1016/S0034-4257(02)00096-2

IPCC (Intergovernmental Panel on Climate Change) (2014) Anthropogenic and Natural Radiative Forcing. In Climate Change 2013 - The Physical Science Basis: Working Group I Contribution to the Fifth Assessment Report of the Intergovernmental Panel on Climate Change, Cambridge: Cambridge University Press, pp. 659–740. https://doi.org/10.1017/CBO9781107415324.018

Jee, J.B., Lee, K.T., Lee, K.H., Zo, I.S. (2020) Development of GK-2A AMI aerosol detection algorithm in the East-Asia

region using Himawari-8 AHI data. Asia-Pacific Journal of Atmospheric Science, 56, 207–223. https://doi.org/10.1007/s13143-019-00156-3

Kaufman, Y.J., Tanré, D., Remer, L.A., Vermote, E.F., Chu, A., Holben, B.N. (1997) Operational remote sensing of tropospheric aerosol over land from EOS moderate resolution imaging spectroradiometer. Journal of Geophysical Research, 102(D14), 17051–17067. https://doi.org/10.1029/96JD03988

Kim, D., Gu, M., Oh, T.-H., Kim, E.-K., Yang, H.-J. (2021) Introduction of the Advanced Meteorological Imager of Geo-Kompsat-2a: In-orbit tests and performance validation. Remote Sensing, 13(7), 1303. https://doi.org/10.3390/rs13071303

King, M.D., Kaufman, Y.J., Tanré, D., Nakajima, T. (1999) Remote sensing of tropospheric aerosols from space: Past, present, and future. Bulletin of the American Meteorological Society, 80, 2229–2259. https://doi.org/10.1175/1520-0477_1999_080_2229_rsotaf_2_0_co_2

Koch, D., Del Genio, A.D. (2010) Black carbon absorption effects on cloud cover, review and synthesis. Atmospheric Chemistry and Physics, 10, 7685–7696. https://doi.org/10.5194/acp-10-7685-2010

Kokhanovsky, A.A., de Leeuw, G. (2009) Satellite aerosol remote sensing over land, Springer-Praxis, Berlin, Heidelberg, 379 pp.

Leck, C., Bigg, E.K. (2005) Source and evolution of the marine aerosol - a new perspective. Geophysical Research Letter, 32, L19803. https://doi.org/10.1029/2005GL023651

Lee, K.H. (2018) Estimation and validation of collection 6 moderate resolution imaging spectroradiometer aerosol products for East Asia. Asian Journal of Atmospheric Environment, 12,193–203. https://doi.org/10.5572/ajae.2018.12.3.193

Lee, K.H., Li, Z., Kim, Y.J., Kokhanovsky, A. (2009) Atmospheric aerosol monitoring from satellite observations: A history of three decades. In Atmospheric and Biological Environmental Monitoring (Kim, Y.J., Platt, U., Gu, M.B. and Iwahashi, H. Eds), Springer, Berlin, Heidelberg, pp. 13–38. https://doi.org/10.1007/978-1-4020-9674-7_2

Levy, R.C., Mattoo, S., Munchak, L.A., Remer, L.A., Sayer, A.M., Hsu, N.C. (2013) The Collection 6 MODIS aerosol products over land and ocean. Atmospheric Measurement Techniques, 6, 2989–3034. https://doi.org/10.5194/amt-6-2989-2013

Li, J., Wong, M.S., Lee, K.H., Nichol, J., Chan, P.W. (2021) Review of dust storm detection algorithms for multispectral satellite sensors. Atmospheric Research, 250, 105398. https://doi.org/10.1016/j.atmosres.2020.105398

Liora, N., Poupkou, A., Giannaros, T.M., Kakosimos, K.E., Stein, O., Melas, D. (2016) Impacts of natural emission sources on particle pollution levels in Europe. Atmospheric Environment, 137, 171–185. https://doi.org/10.1016/j.atmosenv.2016.04.040

Lohmann, U., Feichter, J. (2005) Global indirect aerosol effects: A review. Atmospheric Chemistry and Physics, 5, 715–737. https://doi.org/10.5194/acp-5-715-2005

McDuffie, E.E., Smith, S.J., O'Rourke, P., Tibrewal, K., Venkataraman, C., Marais, E.A., Zheng, B., Crippa, M., Brauer, M., Martin, R.V. (2020) A global anthropogenic emission inventory of atmospheric pollutants from sector- and fuel-specific sources (1970–2017): an application of the Community Emissions Data System (CEDS). Earth System Science Data, 12, 3413–3442. https://doi.org/10.5194/essd-12-3413-2020

Menon, S., Del Genio, A.D., Kaufman, Y., Bennartz, R., Koch, D., Loeb, N., Orlikowski, D. (2008) Analyzing signatures of aerosol-cloud interactions from satellite retrievals and the GISS GCM to constrain the aerosol indirect effect. Journal of Geophysical Research, 113, D14S22. https://doi.org/10.1029/2007JD009442

Menon, S., Hansen, J., Nazarenko, L., Luo, Y. (2002) Climate effects of black carbon aerosols in China and India. Science, 297(5590), 2250–2253. https://doi.org/10.1126/science.1075159

Mishchenko, M.I., Geogdzhayev, I.V., Cairns, B., Rossow, W.B., Lacis, A.A. (1999) Aerosol retrievals over the ocean by use of channels1 and 2 AVHRR data: sensitivity analysis and Preliminary results. Applied Optics, 38, 7325–7341. https://doi.org/10.1364/AO.38.007325

Myhre, G. (2009) Consistency between satellite-derived and modeled estimates of the direct aerosol effect. Science, 325, 187–190. https://doi.org/10.1126/science.1174461

Nakajima, T., Yoon, S.-C., Ramanathan, V., Shi, G.-Y., Takemura, T., Higurashi, A., Takamura, T., Aoki, K., Sohn, B.-J., Kim, S.-W., Tsuruta, H., Sugimoto, N., Shimizu, A., Tanimoto, H., Sawa, Y., Lin, N.-H., Lee, C.-T., Goto, D., Schutgens, N. (2007) Overview of the Atmospheric Brown Cloud East Asian Regional Experiment 2005 and a study of the aerosol direct radiative forcing in east Asia. Journal of Geophysical Research, 112(D24), D24S91. https://doi.org/10.1029/2007jd009009

Pagano, T.S., Durham, R.M. (1993) Moderate Resolution Imaging Spectroradiometer (MODIS). Proceedings of SPIE 1939, Sensor Systems for the Early Earth Observing System Platforms, (25 August 1993). https://doi.org/10.1117/12.152835

Peyridieu, S., Chédin, A., Tanré, D., Capelle, V., Pierangelo, C., Lamquin, N., Armante, R. (2010) Saharan dust infrared optical depth and altitude retrieved from AIRS: a focus over North Atlantic - comparison to MODIS and CALIPSO. Atmospheric Chemistry and Physics, 10(4), 1953–1967. https://doi.org/10.5194/acp-10-1953-2010

Ramanathan, V., Chung, C., Kim, D., Bettge, T., Buja, L., Kiehl, J.T., Washington, W.M., Fu, Q., Sikka, D.R., Wild, M. (2005) Atmospheric brown clouds: Impacts on South Asian climate and hydrological cycle. Proceedings of the National Academy of Sciences, 102(15), 5326–5333. https://doi.org/10.1073/pnas.0500656102

Ramanathan, V., Crutzen, P.J., Kiehl, J.T., Rosenfeld, D. (2001) Aerosols, Climate, and the Hydrological Cycle. Science, 294, 2119–2124. https://doi.org/10.1126/science.1064034

Rao, C.R.N., McClain, E.P., Stowe, L.L. (1989) Remote sensing of aerosols over the oceans using AVHRR data theory, practice, and applications. International Journal of Remote Sensing, 10(4–5),743–749. https://doi.org/10.1080/014311

68908903915
Reddington, C.L., Conibear, L., Knote, C., Silver, B.J., Li, Y.J., Chan, C.K., Arnold, S.R., Spracklen, D.V. (2019) Exploring the impacts of anthropogenic emission sectors on $PM_{2.5}$ and human health in South and East Asia. Atmospheric Chemistry and Physics, 19, 11887–11910. https://doi.org/10.5194/acp-19-11887-2019
Remer, L.A., Kaufman, Y.J., Tanre, D., Mattoo, S., Chu, D.A., Martins, J.V., Li, R.-R., Ichoku, C., Levy, R.C., Kleidman, R.G., Eck, T.F., Vermote, E., Holben, B.N. (2005) The MODIS aerosol algorithm, products and validation. Journal of Atmospheric Science, 62, 947–973. https://doi.org/10.1175/JAS3385.1
Ross, A.D., Holz, R.E., Quinn, G., Reid, J.S., Xian, P., Turk, F.J., Posselt, D.J. (2018) Exploring the first aerosol indirect effect over Southeast Asia using a 10-year collocated MODIS, CALIPSO, and model dataset. Atmospheric Chemistry and Physics, 18, 12747–12764. https://doi.org/10.5194/acp-18-12747-2018
Schmit, T.J., Griffith, P., Gunshor, M.M., Daniels, J.M., Goodman, S.J., Lebair, W.J. (2017) A Closer look at the ABI on the GOES-R series. Bulletin of the American Meteorological Society, 98, 681–698. https://doi.org/10.1175/BAMS-D-15-00230.1
Schmit, T.J., Gunshor, M.M., Menzel, W.P., Gurka, J.J., Li, J., Bachmeier, S.A. (2005) Introducing the next-generation Advanced Baseline Imager on GOES-R. Bulletin of the American Meteorological Society, 86(8), 1079–1096. https://doi.org/10.1175/bams-86-8-1079
Seinfeld, J.H., Bretherton, C., Carslaw, K.S., Coe, H., DeMott, P.J., Dunlea, E.J., Feingold, G., Ghan, S., Guenther, A.B., Kahn, R., Kraucunas, I., Kreidenweis, S.M., Molina, M.J., Nenes, A., Penner, J.E., Prather, K.A., Ramanathan, V., Ramaswamy, V., Rasch, P.J., Ravishankara, A.R., Rosenfeld, D., Stephens, G., Wood, R. (2016) Improving our fundamental understanding of the role of aerosol-cloud interactions in the climate system. Proceedings of the National Academy of Sciences, 113(21), 5781–5790. https://doi.org/10.1073/pnas.1514043113
Stowe, L.L. (1991) Cloud and aerosol products at NOAA/NESDIS. Global and Planetary Change, 4(1–3), 25–32. https://doi.org/10.1016/0921-8181(91)90066-6
Stowe, L.L., Ignatov, A.M., Singh, R.R. (1997) Development, validation, and potential enhancements to the second-generation operational aerosol product at the National Environmental Satellite, Data, and Information Service of the National Oceanic and Atmospheric Administration. Journal of Geophysical Research, 102, 16923–16934. https://doi.org/10.1029/96JD02132
Tan, I., Oreopoulos, L., Cho, N. (2019) The role of thermodynamic phase shifts in cloud optical depth variations with temperature. Geophysical Research Letters, 46, 4502–4511. https://doi.org/10.1029/2018GL081590
Torres, O., Bhartia, P.K., Herman, J.R., Sinyuk, A., Holben, B. (2002) A long term record of aerosol optical thickness from TOMS observations and comparison to AERONET measurements. Journal of the Atmospheric Sciences, 59, 398–413. https://doi.org/10.1175/1520-0469_2002_059_0398_altroa_2.0.co_2
Vallina, S.M., Simó, R. (2007) Strong relationship between DMS and the solar radiation dose over the global ocean. Science, 315, 506–508. https://doi.org/10.1126/SCIENCE.1133680
von Hoyningen-Huene, W., Kokhanovsky, A.A., Burrows, J.P., Bruniquel-Pinel, V., Regner, P., Baret, F. (2006) Simultaneous determination of aerosol and surface chracteristics from MERIS top-of-atmosphere reflectance. Advances in Space Research, 37, 2172–2177. https://doi.org/10.1016/j.asr.2006.03.017
von Hoyningen-Huene, W., Kokhanovsky, A.A., Wuttke, M., Buchwitz, M., Noel, S., Gerilowski, K., Burrows, J.P., Latter, B., Siddans, R., Kerridge, B.J. (2005) Validation of SCIAMACHY top-of-atmosphere reflectance for aerosol remote sensing using MERIS L1 data. Atmospheric Chemistry and Physics, 6, 673–699. https://doi.org/10.5194/acp-7-97-2007
Wen, S., Rose, W.I. (1994) Retrieval of sizes and total masses of particles in volcanic clouds using AVHRR bands 4 and 5. Journal of Geophysical Research: Atmospheres, 99(D3), 5421–5431. https://doi.org/10.1029/93JD03340
Zhang, P., Lu, N.-M., Hu, X.-Q., Dong, C.-H. (2006) Identification and physical retrieval of dust storm using three MODIS thermal IR channels. Global and Planetary Change, 52(1–4), 197–206. https://doi.org/10.1016/j.gloplacha.2006.02.014
Zhu, T., Melamed, M.L., Parrish, D., Gauss, M., Klenner, L.G., Lawrence, M.G., Konare, A., Liousse, C. (2012) WMO/IGAC Impacts of Megacities on Air Pollution and Climate. Geneva: World Meteorological Organization, Geneva, Switzerland. p. 299.